

SYNTHESIS OF TITANIA NANOTUBE ARRAYS BY ANODIZATION

Ahmed El Ruby Mohamed and Sohrab Rohani
Department of Chemical and Biochemical Engineering, The University of Western Ontario,
London, Ontario, N6A 5B9, Canada. srohani@uwo.ca

Titania nanotube arrays were synthesized in glycerol, ethylene glycol and aqueous solution of carboxymethyl cellulose as base materials. The effects of anodization voltage and time, as well as chemical composition of the electrolyte bath were studied. Nanotube arrays with an inner diameter ranging from 16 to 91 nm, and wall thickness ranging from 7 to 29 nm were fabricated in a glycerol-water electrolyte. Water content of 5 wt% or higher was found to be essential for nanotubes fabrication in glycerol electrolyte. Using modified ethylene glycol (containing 2 wt % and 0.5 wt % NH_4F) instead of glycerol, resulted in nanotube length up to 430 nm after 1.5 hr anodization time. By increasing anodization time to 12 hrs, 19.5 μm long titania nanotube arrays were fabricated in ethylene glycol with a high aspect ratio (length to diameter ratio) of 453. Nanotube arrays were also successfully fabricated in 2 wt % sodium carboxymethyl cellulose aqueous electrolyte (CMC electrolyte). These nanotube arrays had an inner diameter of 42 nm similar to those fabricated in 2 wt % urea-ethylene glycol electrolyte but their length was 450 nm. Nanostructure, phase and chemical composition were investigated by FESEM, XRD and XPS spectroscopy, respectively.

1. INTRODUCTION

In the last decade, low-dimensional nanostructural materials have attracted increasing scientific and technological attention due to their physical properties and their potential applications (Fujishima and Honda, 1972). Dimensionality has a crucial role in determining the properties and performance of nanomaterials. Therefore, the control of size and shape of nanomaterials is of great importance. In contrast to size control, control of the shape of nanostructural materials is more difficult and challenging. The tubes, flakes or wires in the nanoscale region possess novel properties. The discovery of carbon nanotubes by Iijima (1991) with their diverse interesting properties has motivated the quest for the synthesis of nanotubular structures of other substances and chemical compounds such as V_2O_5 , SiO_2 , TiO_2 , Fe_2O_3 , ZrO_2 and MoO_3 . Among these materials, titanium dioxide (titania) has attracted great interest since the discovery of its photosensitivity by Fujishima and Honda, (1972) and due to its strong photo-oxidizing potential, high chemical stability, non-toxicity and low cost (Guozhong, 2004). Titania nanotubes have improved properties compared to other forms of titania for applications in water and air purification photocatalysis, sensing, water photoelectrolysis for hydrogen generation, photovoltaics, photoelectrochemical solar cells (Mor et al., 2006; Shen et al., 2006; Macak et al., 2006), electronics, optics (Premchand, 2006), tissue engineering and molecular filtration (Hueso and Mathur, 2004 and Law et al., 2005). The widespread technological use of titania is impaired by its wide band-gap (3 eV for anatase phase and 3.2 eV for rutile phase), which requires ultraviolet (UV) irradiation for photocatalytic activation. Because UV spectrum accounts for only a small fraction (8%) of the solar spectrum compared to visible light (45%), any shift in the light absorbance of titania from the UV towards visible spectrum region will improve the photocatalytic and photoelectrochemical utility of the material. Titania band gap can be narrowed by doping with different nonmetal ions such as N, C and S and metal ions such as Fe, Mo, Ru, Os and V (Shen et al., 2006; Wu et al., 2005; Yuan and Su, 2004). Titania nanotubes, and nanotube arrays, have been produced by a variety of methods including deposition into a nanoporous alumina template (Hoyer, 1996), sol-gel (Zhang et al., 2001), and hydrothermal processes (Bavykin et al., 2004). However, among these nanotubes fabrication routes, the electrochemical anodization method has attracted the most interest due to its ability to produce integrative, vertically-oriented highly ordered nanotube arrays with controllable dimensions (Mor et al., 2003; Gong et al., 2000; Zhao et al., 2005). In contrast to random nanoparticle systems where slow electron diffusion typically limits their performance (Hueso and Mathur, 2004), the precisely oriented nature of the crystalline nanotube arrays makes them excellent electron percolation pathways for the vertical transfer of electrical

charges across the length of nanotubes (Frank et al., 2004). In addition, the nanotube-array architecture is able to influence the absorption and propagation of light through the architecture by precisely designing and controlling the nanotube internal diameter, wall thickness, and length (Paulose et al., 2006). This study aims at investigation of the effect of different anodization parameters on titania nanotubes morphology fabricated in aqueous glycerol, ethylene glycol and CMC based electrolytes.

2. EXPERIMENTAL SETUP AND METHODS

The experiments were carried out in an electrochemical cell where the two electrodes were placed 4 cm apart (see Figure 1). Titanium foil, over which titania nanotubes were grown, was used as anode while platinum foil was the counter electrode. A direct current power supply (Bio-Rad Laboratories, model 400, Irvine, CA) was employed as a source of constant potential. The DC power supply was equipped with a data acquisition system and a state-of-the-art algorithm and interface for real time monitoring of electrical current and voltage during the experiments. An ultrasonic bath was used for degreasing of titanium foil and final cleaning of fabricated nanotubes. The ultrasonic waves were also used for agitation of the electrolyte during the anodization process to improve the quality of nanotubes by mixing at microscopic level. The pH of the electrolyte was measured using an Orion 5-star plus Benchtop multimeter (Thermoelectron Corp., Waltham, MA). All experiments were carried out at room temperature around 25 °C. The morphology of titania nanotube arrays was studied using Hitachi S 4500 field emission SEM. The cross sectional images were taken on mechanically bent samples where titania nanotube layers were liberated from the supporting Ti foil. All experiments were carried out under a fume hood.

Titanium foil (0.89 mm thick, 99.7% purity, Alfa Aesar, Ward Hill, MA) was cut into 1.4 cm diameter discs. The Ti disc was mounted in a Teflon holder so that only one face of it was exposed to the electrolyte. Glycerol (A. R., 99.5%, Caledon Laboratory Ltd., Georgetown, ON), ethylene glycol 99.5 % with water residual ~ 0.4%. (Caledon Laboratory Ltd., Georgetown, ON), NH_4F , NH_4NO_3 , urea (All three chemicals were A. R. 98 %, J. T. Baker purchased from Mallinckrodt Baker Inc., Phillipsburg, NJ) and deionized water were used in the experiments without any further treatment. Titanium foil discs were degreased by sonication in methanol followed by rinsing with deionized water. Then, they were chemically polished in nitric and hydrofluoric acids solution (5.6 M and 3.3 M, respectively) for 10 sec.

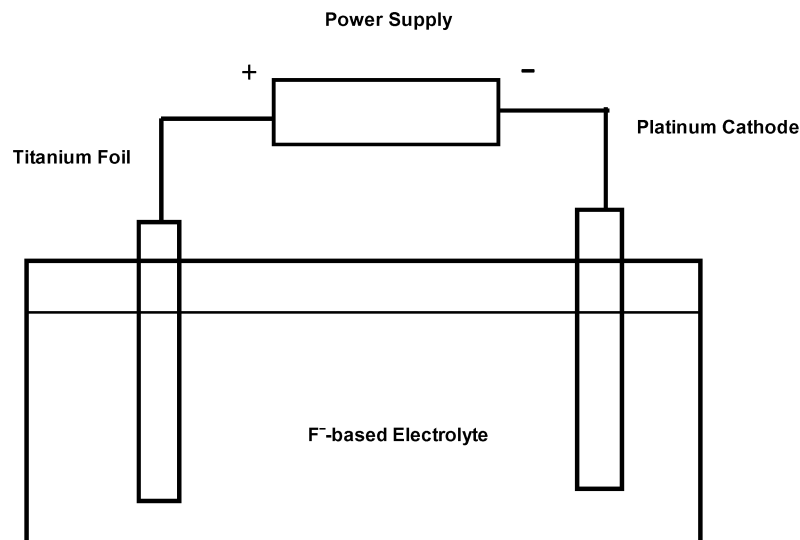


Figure 1: Schematic drawing of an electrochemical cell in which the Ti electrode is anodized.

3. RESULTS AND DISCUSSION

3.1. Glycerol Electrolyte

Titania nanotubes were fabricated at different conditions in glycerol-based electrolytes and the effects of voltage, pH, water content and anodization time were investigated. In general in the absence of water in electrolytes, the anodization process will suffer from lack of H^+ ions and also high viscosity of the solution which leads to the formation of titanium dioxide layers only. The overall reaction for anodic oxidation of titanium can be represented as (Mor et al., 2006):



In the initial stages of the anodization process, field-assisted dissolution dominates chemical dissolution due to the relatively large electric field across the thin oxide layer (the resistance to the current is minimum). Small pits formed due to the localized dissolution of the oxide, represented by the following reaction, act as pore forming centres:



The pits convert to bigger pores and the pore density increases. Subsequently, the pores spread uniformly over the surface. The pore growth occurs due to the inward movement of the oxide layer at the pore bottom (barrier layer). Several anodization experiments were conducted to study the effect of voltage on synthesis and nanoarchitecture at the following conditions: pH: 6, water content: 16 wt%, anodization time: 1.5 hr. Typical results are shown in Figure 2. Increasing anodization voltage from 5 to 40 V increased both the internal diameter and wall thickness of titania nanotube arrays from 16 and 7 nm to 91 and 29 nm, respectively. But at voltage 40 V, titania nanotubes formed only at the edge of the sample while at the center, only shallow pores appeared (see Figure 2: e and f). The discontinuity could be attributed to the field-assisted high dissolution rate at high voltages.

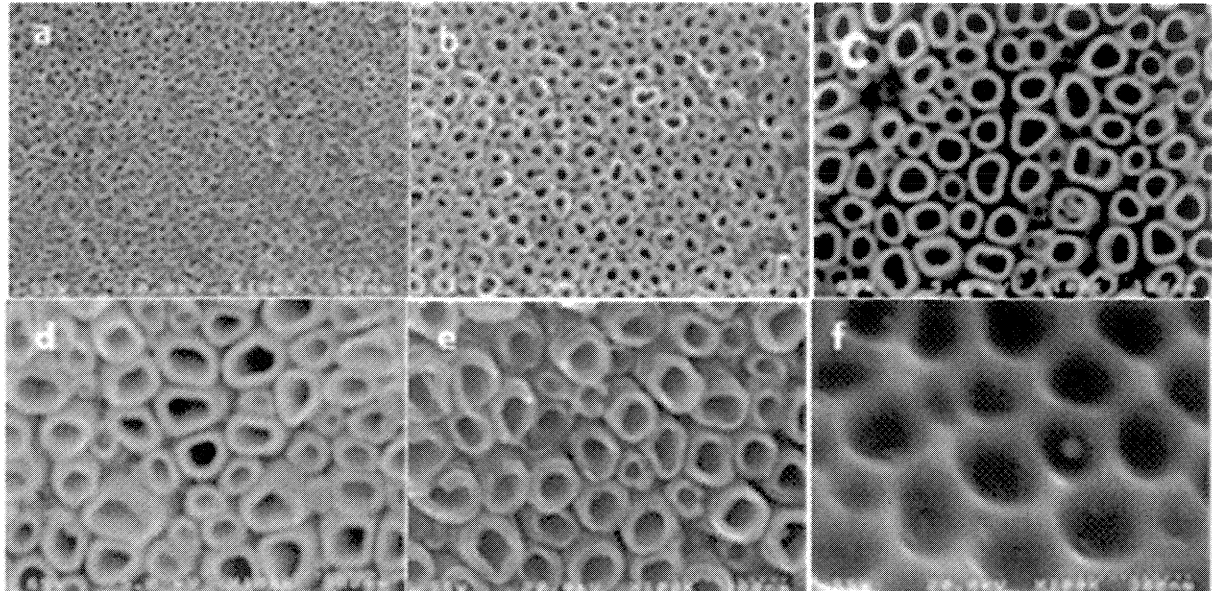


Figure 2: Scanning electron micrographs of the synthesized titania nanotube arrays at different voltage: a) 5V, b) 10V, c) 20V, d) 30V, e) 40V at sample edge, and f) 40V at sample center.

Table 1: Effect of water content on nanotube arrays formation and their nanoarchitecture (20 volts, pH: 6, 0.5 wt% NH₄F and 1.5 hr anodization time)

Water content, wt. %	0	2	5	16	30	50	70	90	100
Diameter, nm	n/a*	n/a*	38	64	76	72	48	43	40
Wall thickness, nm	n/a*	n/a*	18	20	20	18	13	12	14
Length, nm	n/a*	n/a*	-	250	512	900	533	460	424

* not applicable

Potential window for nanotubes fabrication in glycerol appears to be wider than acidic aqueous electrolyte where achieving titania nanotube arrays below 10 V and above 25 V was not possible (Cai et al, 2005). In general, in the absence of water in electrolytes, the anodization process will suffer from lack of H⁺ ions and also high viscosity of the solution which leads to the formation of titanium dioxide layers only. It was found that the presence of a small amount of water in organic electrolyte was essential to form nanotubular structure (Raja et al., 2007). Table 1 shows the effect of different water contents at 20 volts, pH: 6 and anodization time 1.5 hr. At 0 or 2 wt% water content, no nanotube arrays were formed. Nanotube arrays began to form at 5 wt% water content and increasing water content from 5 wt% to 50 wt% affected the nanoarchitecture of nanotube arrays where the diameter increased from 38 to 76 nm and nanotube length increased from 250 to 900 nm when increased the water content from 16 to 50 wt%. Further increase of water content to 99.5 wt% (0 % glycerol) led to a decrease in nanotube diameter and length to 40 nm and 424 nm, respectively. The increase of diameter and length with water content in the range from 5 to 50 wt% can be explained by the electrolyte viscosity role. There are two competing rate processes: The tube growth at the bottom of the tube and the rate of chemical dissolution of the tubes at the top of nanotubes. Both processes are affected by the viscosity of the electrolyte and the rate of diffusion of different ions through it. At low water content the viscosity is very high and this results in high H⁺ ion concentration gradient between the bottom and top of the nanotubes. H⁺ ions high concentration at the bottom of nanotubes increase the rate of oxidation reaction and, consequently, the building rate of nanotubes. Low concentration of H⁺ ions at the nanotubes top reduces the dissolution rate of nanotube walls. While at the same time, low diffusion rate of reactant species such as F⁻ ions and reaction products such as TiF₆⁻ from the bottom of nanotubes to the bulk of the electrolyte constrains the overall reaction rate. The net result of pH gradient effect and the diffusion rate effect determines the overall effect of electrolyte viscosity. The pH gradient across the nanotube length is very high at low water content and decreases with increasing water content in glycerol electrolyte. On the other hand, the diffusion constraint on the reaction rate decreases by increasing water content and the oxidation reaction rate increases with increasing water content. The net effect of these two competing processes resulted in the optimum water content of 50 wt% at which maximum length and inner diameter of 900 and 76 nm, respectively, were achieved as shown in Table 1.

A few minutes are needed in aqueous electrolytes for the preliminary development of the nanotubular structures [Cai et al., 2006]. This is followed by an increase of the length of nanotubes. The growth of nanotube length is time dependent and the time dependence differs according to the composition of electrolyte bath. For the strong acidic HF – water based electrolytes; the nanotube length is time independent after the first hour because the rate of chemical dissolution at the top of nanotubes equals the rate of nanotubes formation at the bottom of the tubes. Under these conditions, the length is limited to about 500 nm and further increase in anodization time does not increase the nanotube length. For aqueous electrolytes with near-neutral pH, the maximum nanotube length reported was 4.4 μm after 20 hrs [Cai et al., 2005]. Macak and Schmuki, 2006, studied the effect of time on nanotube length in two electrolyte baths: (1) glycerol + 0.5 wt% NH₄F and (2) 1 M NH₄SO₄ + 0.5 wt% NH₄F in water. For the first electrolyte they found that the length increased almost linearly with time until it reached 6 μm after 18 hr (nanotube length was time-dependent), while in the second electrolyte, the length reached its maximum value of about 2.5 μm after 2 hr and after that the nanotube length was time-independent for the rest of the 18 hr. They also found that the rate of growth of nanotube length in water-based electrolyte was higher than in glycerol-based electrolyte in the first 2 hr which could be attributed to the high viscosity of the glycerol electrolyte.

In the present study, several anodization experiments were conducted at pH: 10 V and 16 wt% water content and different anodization times. Figure 3 indicates that increasing the anodization time affected neither nanotube

diameter nor wall thickness and they remained approximately constant at 30 and 13 nm, respectively. But the nanotubes length increased from 200 nm to 470 nm when anodization time increased from 0.5 hr to 10 hr. It is worth-mentioning that by increasing the voltage from 10 to 20 volts and water content from 16 to 50 wt %, nanotube arrays with length of 900 nm were obtained after only 1.5 hr. This implies that longer nanotubes can be formed by increasing anodization time. It is desirable to have longer continuous nanotubes as the photocurrent intensity increases with increasing the tube length. The results of this study agree with other research works which showed that the diameter and wall thickness of nanotube arrays are independent of anodization time when other anodization conditions are kept constant (Mor et al., 2006). The results show that the length of nanotubes is time-dependent at high pH values (pH around 6). This is because at high pH, the growth rate of nanotubular oxide layer at metal/oxide interface is much higher than the dissolution rate of TiO₂ nanotubes at the oxide/electrolyte interface (Cai et al., 2005).

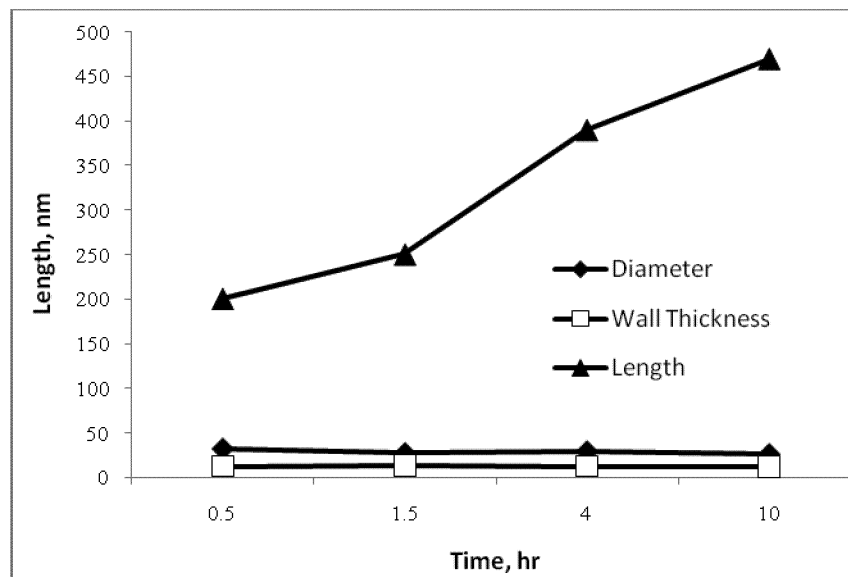


Figure 3: Effect of anodization time on length, diameter and wall thickness of titania nanotubes fabricated at 10 V, 16 wt% water content, pH: 6 and 0.5 wt% H₄F

3.2. Ethylene Glycol Electrolyte

As mentioned earlier, viscosity of the electrolyte has a direct impact on diffusion of reactants and products to and from the titania nanotubes surface. It is necessary to control diffusion for synthesis of well organized titania nanotubes, however, there is a certain range beyond which the viscosity has negative impact on synthesis and growth rate of titania nanotubes. The growth rate was low in glycerol-based ($\eta = 945$ cP at 25 °C) electrolytes and addition of water improved the growth rate due to the reduction in the viscosity of electrolyte solution. Ethylene glycol is less viscous ($\eta = 16$ cP at 25 °C) compared to glycerol and results in lower diffusion resistance. Therefore, the growth rate would be higher in ethylene glycol electrolytes. Parameters that were previously studied in glycerol experiments were fixed at 20 volt, 1.5 hr, pH: 6 and water content was kept at only the residual amount (~ 0.4 wt %). Urea and NH₄NO₃ were added to study their effect on nanotubes morphology and as additional sources for nitrogen doping into the nanotubes. Results in Table 2 show that adding 1 wt% urea increased nanotube length from 286 nm to 397 nm (more than 27%) and adding 2 wt% urea increased the nanotube length to 430 nm (50 % increase). Adding 1-2 wt% urea increased the nanotube diameter from 30 nm to around 40 nm and thickness from 11 nm to 18 nm. Urea is likely to have an inhibitory effect on acid corrosion of metals in the presence of halide ions. Adding 1 wt% ammonium nitrate increased the nanotube length from 286 to 365 nm (21 % increase) while adding 2 wt% ammonium nitrate to the electrolyte increased the length to 320 nm. This increase in nanotubes length in the presence of ammonium nitrate was attributed to

the increase of electrolyte conductivity by addition of this ionic compound. Increasing anodization time from 1.5 hrs to 12 hrs while keeping all other parameter fixed as experiment 5 in Table 2, resulted in increasing nanotubes length to $\sim 19.5 \mu\text{m}$ with a high aspect ratio of 453 (the ratio between nanotubes length to nanotubes diameter). Figure 4 shows a SEM images of the nanotube arrays fabricated in ethylene glycol electrolyte: a) top view, b) bottom view, c) Cross-section view of sample anodized for 12 hrs at the same conditions as for experiment 5 in Table 2, d) cross-section at high magnification showing smooth nanotube walls while the higher magnification, the insert (e), shows that there are periodic rings cementing the nanotubes to each other which help increasing the mechanical strength of the nanotube arrays.

Experiment #	Urea, wt.%	NH_4NO_3 , wt.%	TNTAs* length, nm	TNTAs* Diameter, nm	Wall thickness, nm
1	0	0	286	30	11
2	0	1	365	28	11
3	0	2	320	33	9
4	1	0	397	40	18
5	2	0	430	43	16

* TNTAs: Titania nanotube arrays.

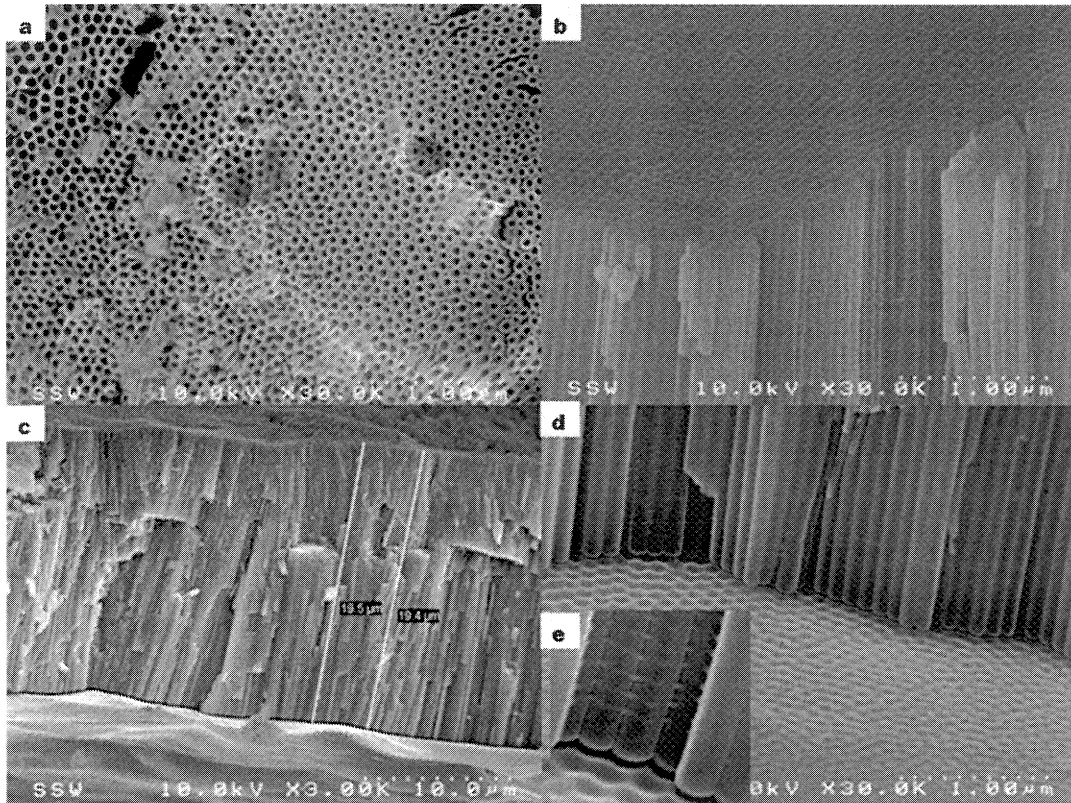


Figure 4: SEM images of TiO_2 nanotube arrays fabricated in ethylene glycol-based electrolyte at conditions as experiment 5 in table 2.: a) Top view, b) bottom view, c) cross-section of sample anodized for 12 hrs showing very long nanotubes and d) cross-section at high magnification showing smooth nanotube walls and e) (inset) more higher magnification of (d) showing the presence of periodic rings connecting the outer surfaces of the nanotubes.

3.3. Anodization in CMC Aqueous Electrolyte

Due to the high cost of glycerol and ethylene glycol as viscous electrolytes for Ti anodization, preliminary investigation of nanotube arrays fabrication in sodium methyl carboxycellulose (CMC) aqueous solutions was conducted. The use of CMC-based electrolyte for the anodization of titania is not reported in the literature. We were able to fabricate nanotube arrays by Ti anodization in CMC aqueous electrolyte. Figure 5 shows the SEM images of titania nanotube arrays fabricated at 20 volts, 2 wt% CMC aqueous electrolyte, 0.5 wt% NH_4F , and pH: 6 and anodization time 1.5 hr. The nanotubes length was 450 nm and the average diameter was 42 nm at 20 volts and 28 nm at 10 volts, which assures the trend of diameter increase with increasing voltage. Figure 5 shows a comparison between 7 different electrolyte compositions in terms of length and diameter of the nanotube arrays anodized at 20 V, pH: 6, 0.5 wt% NH_4F and anodization time: 1.5 hrs. The electrolyte compositions are as follows: (1)- Water: 0.5wt% NH_4F in water, (2)- Gl (16% H_2O): 16wt% water in Glycerol, (3)- Gl (Glycerol): H_2O : 1:1 (wt/wt), (4)- Ethylene glycol (EG), (5)- 2 wt % Ammonium Nitrate in EG, (6)- 2 wt% urea in EG and (7)- 2 wt% CMC aqueous solution. As it can be easily seen from the histogram in Figure 6, maximum nanotube length and diameter were obtained from 50 wt% water in glycerol. Nanotubes anodized in CMC electrolyte have almost the same diameter as those anodized in ethylene glycol (2 wt % urea) electrolyte and those anodized in aqueous electrolyte (0 % glycerol) but the length of CMC –nanotubes was slightly higher than the nanotube length obtained from those both electrolytes. Also, CMC-nanotubes length was 80 % longer than the nanotube length obtained from 16 wt % water in glycerol.

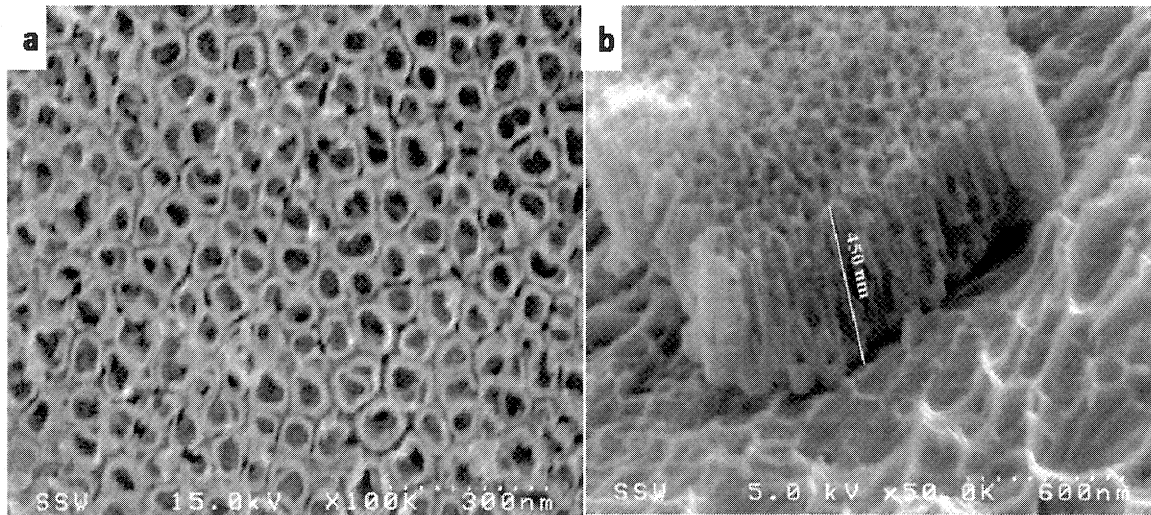


Figure 5: SEM image of titania nanotube arrays fabricated in 2 wt % CMC aqueous solution at 20 V, pH: 6, 0.5 wt % NH_4F , and 1.5 hr. a) top view and b) cross sectional view.

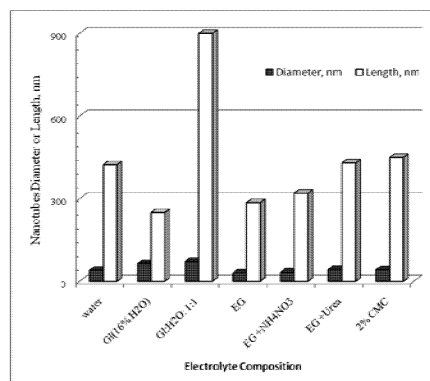


Figure 6: Comparison among different electrolyte compositions in terms of diameter and length of nanotubes (see electrolyte composition details in text).

3.4. XRD and XPS Characterization of Titania Nanotube Arrays

The as-anodized TiO₂ nanotube arrays are amorphous. Annealing TiO₂ nanotube arrays convert them to crystalline phase either to anatase or rutile depending on annealing temperature (Yang et al., 2008). Figure 7 shows X-ray diffraction patterns for two samples annealed at 550 °C and 800 °C for 32 hrs in air. Sample annealed at 550 °C contains both anatase and rutile phases as well as Ti metal in the substrate metal. While sample annealed at 800 °C contained increased amounts of rutile phase and does not contain anatase phase. This is because all anatase phase transformed to rutile phase which is the more stable phase at high temperature in addition to a part of Ti metal in substrate was oxidized at 800 °C in the presence of air. These results were in agreement with previous works (Mor et al, 2006; Yang et al., 2008).

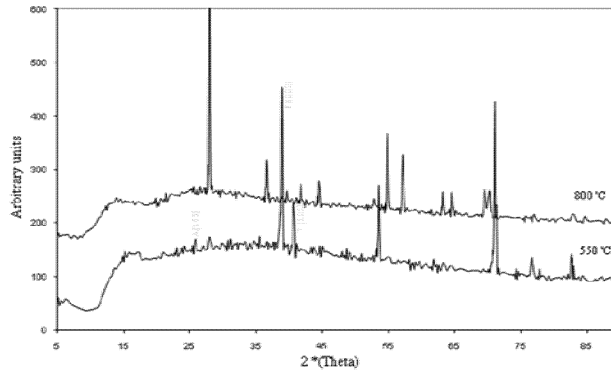


Figure 7: X-ray diffraction patterns for TiO₂ nanotube arrays annealed at 550 °C and 800 °C

Figure 8 shows the XPS spectra of TiO₂ nanotube arrays fabricated in 16% wt % water, 0.5 wt% NH₄F in glycerol for 1.5 hr and annealed at 550 °C in air for 2 hrs. The spectra show that chemical composition of nanotubes is TiO₂ Ti: O atomic ratio is approximately 1:2. The excess in O is attributed to oxygen associated to carbon either from air or as a residual of glycerol from the anodization electrolyte. Although XPS is not a good quantitative tool for measuring carbon at a surface, high resolution XPS scan (not shown here) showed that small quantities of carbon atoms were present either as chemisorbed at the TiO₂ surface or as graphitized carbon and this helps reducing band gap of TiO₂ and enhances the visible light photoactivity of TiO₂ nanotubes (Raja et al., 2006). Figure 8 also shows the presence of 0.9 atom % Nitrogen which help reducing band gap of the TiO₂ nanotubes and consequently increase its photoactivity in visible light region.

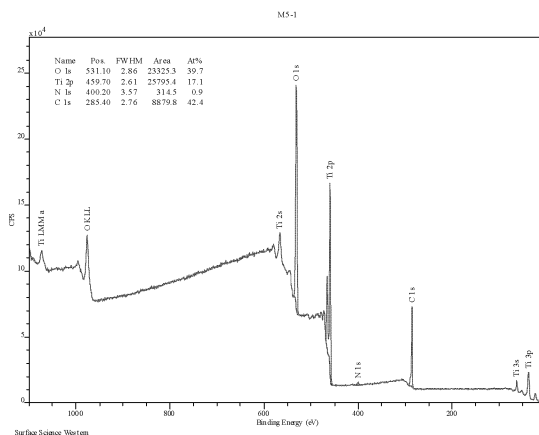


Figure 8: XPS spectra for TiO₂ nanotube arrays fabricated in glycerol-based electrolyte

CONCLUSIONS

Highly ordered titania nanotube arrays were successfully fabricated in glycerol, ethylene glycol and CMC-based electrolytes. Our results showed that synthesis parameters play a crucial role in both nanotube arrays formation and tailoring of their nanoarchitecture. Nanotube arrays with an inside diameter ranging from 16 to 91 nm, and wall thickness ranging from 7 to 29 nm were fabricated in a glycerol-water electrolyte. Water content of at least 5 wt%, was found to be essential for nanotubes fabrication in glycerol electrolyte. Diameter and length were influenced by varying water content above 5 wt%. Using modified ethylene glycol solution instead of glycerol resulted in nanotubes length up to 430 nm after 1.5 hr anodization time in ethylene glycol containing 2 wt % urea and 0.5 wt% NH₄F and by increasing anodization time from 1.5 to 12 hrs while keeping other parameters constant, nanotubes of 19.5 μ m length and aspect ratio of 453 were obtained. Nanotube arrays were successfully fabricated in 2 wt % sodium carboxymethyl cellulose aqueous electrolyte.

REFERENCES

- Bavykin, D. V., Parmon, V. N., Lapkin, A. A. and Walsh, F. C., (2004), *J. Mater. Chem.* 14, 3370.
- Cai, Q., Yang, L. and Yu, Y., (2006), *Thin Solid Films* 515, 1802.
- Cai, Q., Paulose, M., Varghese, O. K. and Grimes, C. A., (2005), *J. Mater. Res.*, 20, 230.
- Frank, A. J., Kopidakis, N. and Van de Lagemaat, J., (2004), *Coord. Chem. Rev.* 248, 1165.
- Fujishima, A. and Honda, K., (1972), *Nature* 238, 37.
- Gong, D., Grimes, C. A., Hu, W., Singh, R. S., Chen, Z. and Dickey, E. C., (2001), *J. Mater. Res.* 16, 3331.
- Guozhong, Cao, (2004), *Nanostructures and Nanomaterials: Synthesis, Properties and Applications*, Imperial College Press p. 15.
- Hoyer, P., (1996), *Langmuir* 12, 1411.
- Hueso, L. and Mathur, N., (2004), *Nature* 427, 301.
- Iijima, S., (1991), *Nature* 354, 56.
- Law, M., Greene, L. E., Johnson, J. C., Saykally, R. and Yang, P. D., (2005), *Nature Materials* 4, 455.
- Macak, J. M. and Schmuki, P., (2006), *Electrochimica Acta* 52, 1258.
- Mor, G. K., Varghese, O. K., Paulose, M., Mukherjee, N. and Grimes, C. A., (2003), *J. Mater. Res.* 18, 2588.
- Mor, G. K., Varghese, O. K., Paulose, M., Shankar, K. and Grimes, C. A., (2006), *Solar Energy Materials & Solar cells* 90, 2011.
- Paulose, M., Shankar, K., Yoriya, S., Prakasam, H. E., Varghese, O. K., Mor, G. K., Latempa, T. A., Fitzgerald, A. and Grimes, C. A., (2006), *J. Physical Chemistry B: Letters* 110, 16179.
- Premchand, Y. D., Djenizian, T., Vacandio, F. and Knauth, P., (2006), *Electrochemistry Communications* 8, 1840.
- Raja, K. S., Ganndhi, T. and Misra, M., (2007), *Electrochemistry Communications* 9, 1069.
- Raja, K. S., Misra, M., Mahajan, V. K., Gandhi, T., Pillai, P. and Mohapatra, S. K., (2006), *J. Power Sources* 161, 1450.
- Shen, Q., Sato, T., Hashimoto, M., Chen, C. and Toyoda, T., (2006), *Thin Solid Films* 499, 299.
- Wu, P., -G., Ma, C. -H. and Shang, J. K., (2005), *Applied Physics A: Material Science & Processing* 81, 1411.
- Yang, Y., Wang, X. and Li, L., (2008), *J. Am. Ceram. Soc.* 91, 2, 632.
- Yuan, Z-Y. and Su, B-L., (2004), *Col Y. colloids and Surfaces A: Physicochem. Eng. Aspects* 241, 173.
- Zhang, M., Brando, Y. and Wada, K., (2001), *J. Mater. Sci. Lett.* 20, 167.
- Zhao, J., Wang, X., Sun, T. and Li, L., (2005), *Nanotechnology* 16, 2450.

